GRID-EDGE-DEPTH MAP BUILDING EMPLOYING SAD WITH SOBEL EDGE DETECTOR

Budi Rahmani[1,2], Agus Harjoko[1], Tri Kuntoro Priyambodo[1]

[1]Department of Computer Science and Electronics, Faculty of Mathematics and Natural Science, Universitas Gadjah Mada, Yogyakarta, Indonesia

[2]Program Studi Teknik Informatika, STMIK Banjarbaru, Kalimantan Selatan, Indonesia

Emails: budirahmani@gmail.com, aharjoko@ugm.ac.id, mastri@ugm.ac.id

Submitted: May 15, 2017 *Accepted: July 17, 2017* *Published: Sep. 1, 2017*

Abstract - This paper presents a new method of a map building which is suitable for a wheeled robot. The 2D map represents the obstacle's position and distance in the environment. The information of the obstacles obtained from a calibrated stereo camera. The stereo images size were 320x240 pixels. Hereafter the images were rectified and the disparity map was built using a Sum of Absolute Difference (SAD) algorithm. The depth map was calculated using disparity map, focal length, and baseline parameter values. In order to detect the obstacles, Sobel edge detection was implemented. The edge detection image was compared and substituted with the depth map which is resulting edge-depth map. The edge-depth map was divided into 25 grids (5 grids horizontal and 5 grids vertical). Finally, the minimum depth of detected obstacles for each grid was calculated. This process was resulting in a grid-edge-depth map (GED map). The proposal has been tested with a mobile robot in 5x3 meters living environment. Finally, experimental results are presented. The average error of feature points in the previous study was 5.40 cm, whereas in this study is 3.82 cm. There has been a decrease in the measurement gap of 29.26% from the previous study.

Index terms: Disparity, grid-edge-depth map, SAD, Sobel, stereo camera, wheeled robot

I. INTRODUCTION

In recent years, mobile robot navigation has been studied as the basic functionality of a robot in living environments such as home or office. Consequently, mobile robot that coexists with people is required to adapt to such environment [1]. In this case, a map of the environment may be used by the mobile robot. Using the map, the robot can localize itself [2], identify the position of the obstacle, and all at once to avoid collisions against these obstacles [3]. Moreover, the map will be useful to give a safe and efficient information of the environment in order to reach a certain place or position. In some cases, maps of environments only present the information of static obstacles position [4]. When the position of one or more obstacles was changed, the map is no longer usable. Consequently, the map needs to be updated periodically [5].

Map building for mobile robot navigation is a generation of an abstract representation of a real environment [6]. Hence to perceive information of environment, ordinarily a mobile robot equipped with sensors [7]. It can be a vision, sonar, or another kind of sensors. Vision-based mobile robot mostly equipped at least with one camera, and others equipped with dual or more camera at the same time [8]. Research has been conducted on building a map of static obstacles, for examples building an unknown outdoor environmental map as [9]. In this case, a local and global map of the environment was developed. The method utilized the point cloud model combined with visual odometry. This combination is used to assist the robot in path planning to the desired location in the outdoor environment [9]. This model was having a shortcoming in the ability of a robot to anticipate changes of the obstacles' position since its only deal with static obstacles.

Another study of environmental mapping algorithm was conducted by [7]. In this approach, a stereo camera was used and mounted on a car. Therefore they built the local disparity map, obstacle analysis, and path planning. The next process of building a map is the V-intercept algorithm. This algorithm affords to detect the obstacles. The detected obstacles are conceived on a cost map. This map is used to plan the navigation path [7].

This paper presents a new approach of a grid-edge-depth map building algorithm. The map is a 2D map of a living environment which represents the obstacle's position and distance. The information of environment obtained from a calibrated low-cost stereo camera mounted on a wheeled robot. The 320x240 pixels of images is used. Disparity map built using a SAD algorithm with 25-pixel block size [10]. The depth map was calculated using disparity map, focal length, and baseline parameter values. In order to detect the obstacles, Sobel edge detection was implemented. The edge detection image was compared and substituted with the depth map which is resulting edge-depth map. The edge-depth map was divided into 25 grids (5 grids horizontal and 5 grids vertical). Finally, the minimum depth of detected obstacles for each grid was calculated. This process was resulting in a grid-edge-depth map (GED map). The proposal has been tested with a mobile robot in 5x3 meters living environment.

II. PROPOSED METHOD

A. Stereo Camera Assembling and Calibration

In this study, our stereo camera consists of two fixed focus cameras (Logitech C270). The cameras were mounted on a 5 mm acrylic respectively. The baseline of stereo camera (the distance of cameras lens) was 7 cm. The distance was the smallest since the camera mounted side by side horizontally. Each camera connected to the computer via USB port. Stereo camera used in this study are shown in Figure 1.

Figure 1. Assembled stereo camera

In order to derive accurate knowledge about the physical dimension and/or location of an observed object, camera calibration is absolutely required [11][12]. The camera calibration is the process of determining the internal camera geometric and optical characteristics (intrinsic parameters) and orientation of the camera frame relative to a certain world coordinate system (extrinsic parameters) [13][14]. In this research, we used camera calibration toolbox by Jean-Yves Bouguet [15], including image rectification, radial undistortion, and tangential undistortion [16]. We used 20 pairs of the 320 x 240 pixels of chessboard image. Figure 2 shows the images that are used in the camera calibration process. Once the intrinsic and extrinsic parameter has obtained after calibration process, the next process is image rectification [17]. Using the parameter we have obtained, radial undistortion and tangential undistortion implemented to acquire images in real-time. Figure 3 shows the unrectified stereo images obtained from our stereo camera. The next step of our proposed algorithm only worked with images which have already been rectified. Image rectification is done only horizontally for matching blocks, and not vertically. In this case, image rectification result shows a feature in the left image will be in the same pixel row in the right image [18].

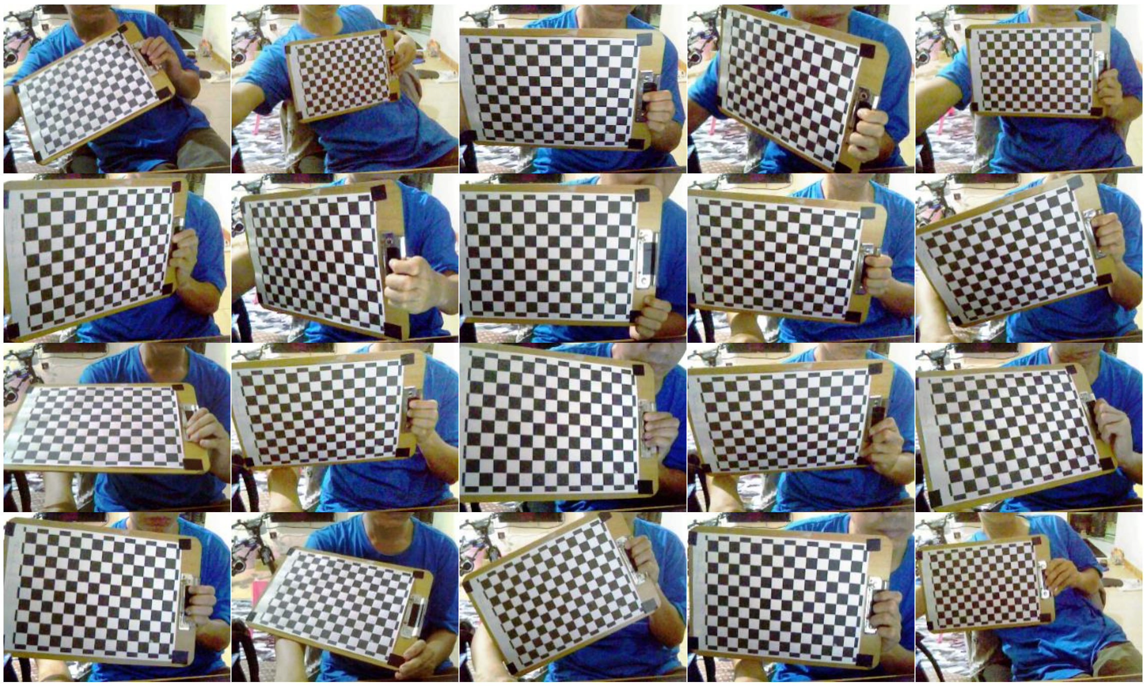

Figure 2. Twenty Images for camera calibration process

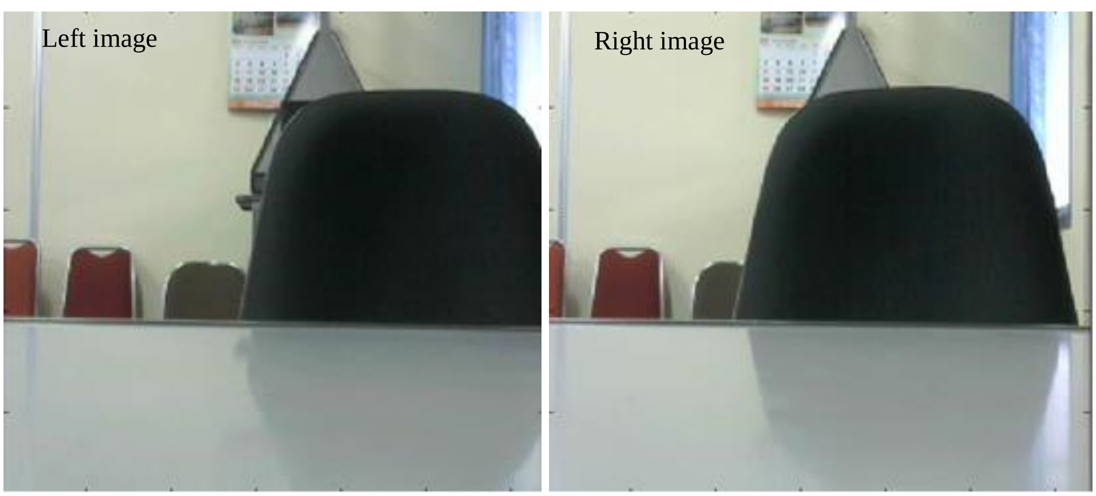

Figure 3. Unrectified left and right images

B. Environment setup

A living room has been used in this study. The environment's purpose was depicted in Figure 4. The obstacles are folding table and side chairs. The dimension was 40 centimeters deep by 20 centimeters wide for the side chairs and 30 centimeters wide by 40 centimeters long by 30 centimeters height respectively. There were 8 side chairs and 9 folding used in our experiment. Subsequently, the experimental environment size is 5 meters long by 3 meters wide. Lighting condition was 600 lumens.

Figure 4. The environment setup

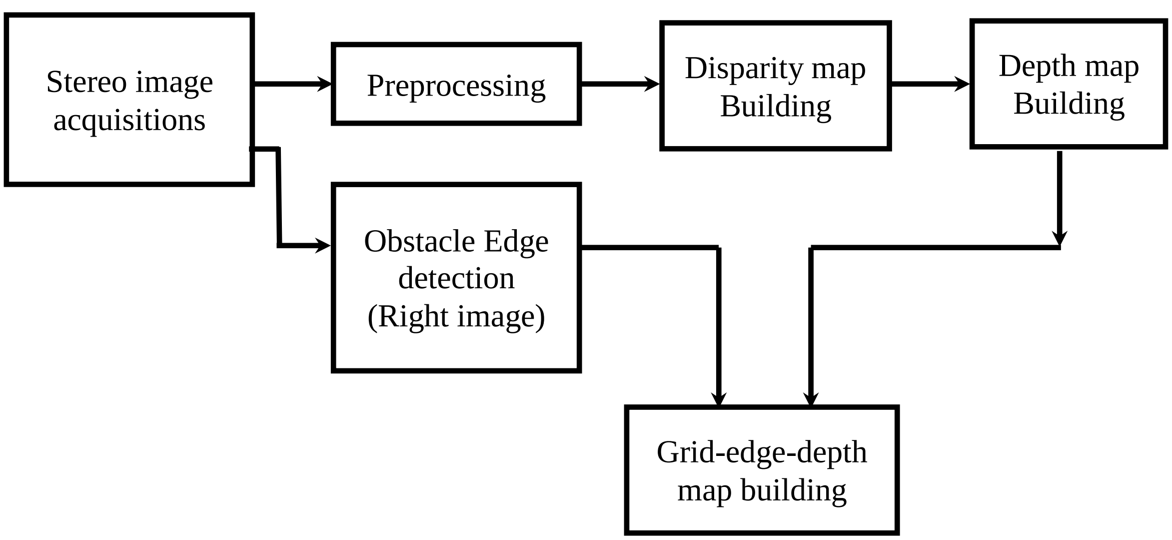

Figure 5. Proposed Model

C. Stereo image acquisitions and preprocessing

Figure 5 shows our proposed model in building a navigation map. We proposed a new approach utilizing edge feature and depth information of the obstacles. The process started from Stereo image acquisitions using calibrated stereo camera. We used the stereo camera since its reliability and high accuracy in measuring the distance of the obstacles. The histogram equalization is applied into acquired stereo images. The RGB color of stereo images converted into the grayscale color space. RGB color space consists of 3 channels which mean that it requires 3 times more computation and memory space compared to grayscale which only consists of one channel [13]. Therefore image rectifications using the camera calibration parameter is done in preprocessing.

D. Disparity map building

In order to obtain a disparity map, Sum of Absolute Difference (SAD) is used. The SAD technique is the common stereo matching algorithms, caused by its low complexity and good result [14] [19]. Equation 1 shows basic SAD algorithm in order to obtain the disparity map. $SAD(x, y, d)$ is disparity image of (x,y) pixels. $I_L(i, j)$ is intensity function of left image on (i,j) coordinate. $I_R(i, j) =$ is intensity function of right image on (i,j) coordinate. $W(x, y)$ is an (x,y) square windows of the disparity map. And d is maximum disparity value. In this study, we used d=48 since it's the best value in order to obtain the distance of obstacles in our environment of the experiment.

$$SAD(x, y, d) = \sum_{(i,j) \epsilon\, W(x,y)} | \, I_L(i, j) - \; I_R(i - d, j) \, | \tag{1}$$

In our case, SAD with block comparison technique is used. And to compute the sum of absolute differences between the template image (left image) and a block on the right image, we subtract each pixel in the template (left image) from the corresponding pixel in the block on the right image. Then the absolute value of the differences could be calculated. These differences pixels then summarized and a single value is derived that roughly measures the similarity between the two images patches. A lower value means the patches (a block pixel from left and right image) are more similar. This technique is shown in Figure 6. Meanwhile, the size of our block is 25 pixels.

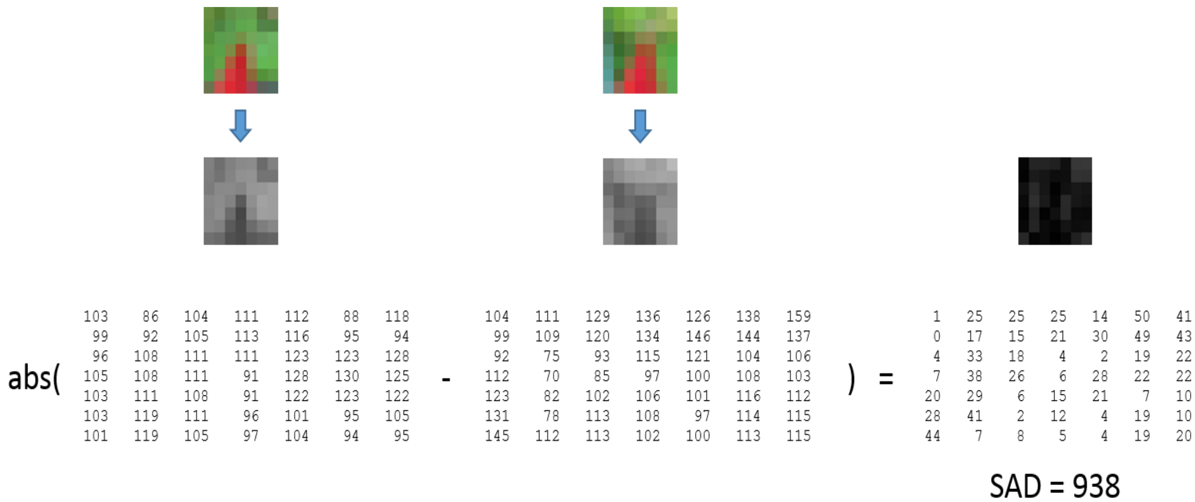

Figure 6. Block SAD matching example [18]

E. Depth map building

Depth map was built based on disparity map [20]. It was derived by calculating the camera baseline and camera focal length. Then it was divided with every pixel of the disparity map. In this study, our stereo camera baseline is 7 cm and our stereo camera focal length is 428 pixels. Equation (2) shows how depth map was calculated.

$$depth_{(row,col)} = \frac{focal\ Length * baseline}{disparitySAD_{(row,col)}} \quad (2)$$

F. Obstacle Edge Detection (right image)

Sobel edge detection algorithm is used in this study. Nevertheless, the Canny algorithm also as popular as Sobel algorithm [21]. Both of them are often used to detect the presence of the obstacles. The Sobel edge detection algorithm is applied to the right image. The right image is used since it is a comparator image in building a disparity map. The result of this process is a binary image. Pixel intensity of the edge of detected obstacle will be one (the color is white), and others will be zero (the color is black) [22]. We used Matlab image processing toolbox for this entire edge detection.

G. Grid-Edge-Depth map building

1. Edge-Depth pixel substitution

In order to obtain depth or distance for every detected obstacle, then the substitution was done. Using the equation (3) Edge-Depth was processed. Every pixel is worth one will be replaced by the value of depth map at the same pixel position. And every zero pixels will be replaced with a value of 500 (farthest object in the experiment environment is 500 cm).

$$EdgeDepth(row, col) = \begin{cases} depthMap, & Edge(row, col) = 1 \\ 500, & Edge(row, col) = 0 \end{cases} \quad (3)$$

In this step, edge depth map was divided into 5 rows and 5 column (25 grids). The row and the column size for each grid were 48 and 64 pixels respectively since the size of edge depth map was 320x240 pixel.

2. Minimal Grid-Edge-Depth

In order to obtain the distance of each grid, we calculate the minimum value of the depth of each grid. This minimum value is the nearest distance of detected obstacle's edge. For navigation reason, this nearest distance will be awarded as an obstacle. The next step, the robot will make a decision for this condition.

III. EXPERIMENTAL RESULTS AND ANALYSIS

The proposed method is applied to build a map in a living environment. The performance of our method is evaluated by comparing the real distance and minimum grid distance of detected object. The results of experiments of this study have depicted on Figure 7, Figure 8, Figure 9, and Figure 10, respectively. In Figure 7 shown in the initial left and right images that are acquired using the stereo camera. Hereinafter, we applied histogram equalization on the acquired stereo images. The results of this process shown in Figure 8. Further, the stereo images converted into the grayscale color space, and the proceeds are shown in Figure 9. Furthermore, Figure 10 shown in the rectified left and right images of two difference scene, then result in the process of edge detection of the right image using Sobel operator for each scene.

Hereinafter, Figure 11 shows the disparity map of SAD building block matching algorithm and calculated depth map according to focal length and baseline value of the stereo camera calibration. In this paper, our focal length is 428 pixel and the baseline is 7 cm. Disparity values that are used in building the disparity map are 48, according to the equation 1. This value is set after testing the disparity value from 0 to 64 with the interval equal to 16. Meanwhile, the block size used was 25 pixels. This is the best block size in this paper in order to reach the minimum and the maximum object distance measurement.Based on the experiment, the minimum distance could be calculated by the program is 63 cm. If the disparity value equal to 64, then minimum distance could be measured by the program become 50 cm. Unfortunately, the maximum distance could be measured is not more than 200 cm.

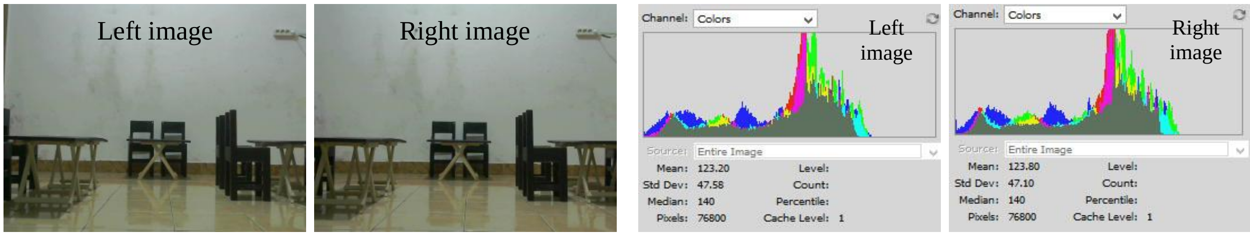

Figure 7. Initial left and right images and its histogram

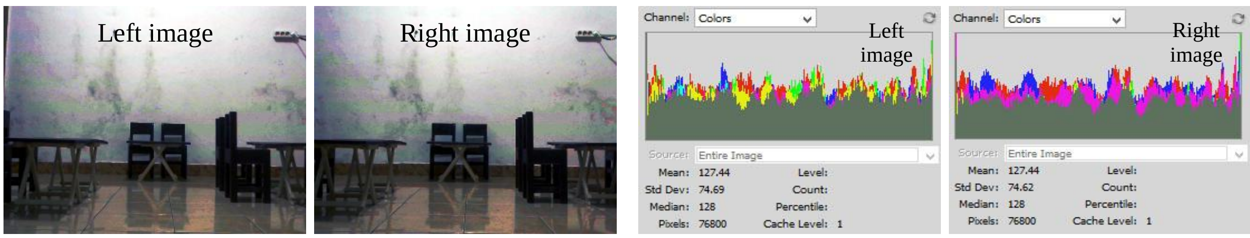

Figure 8. Left and right images after histogram equalization and its histogram

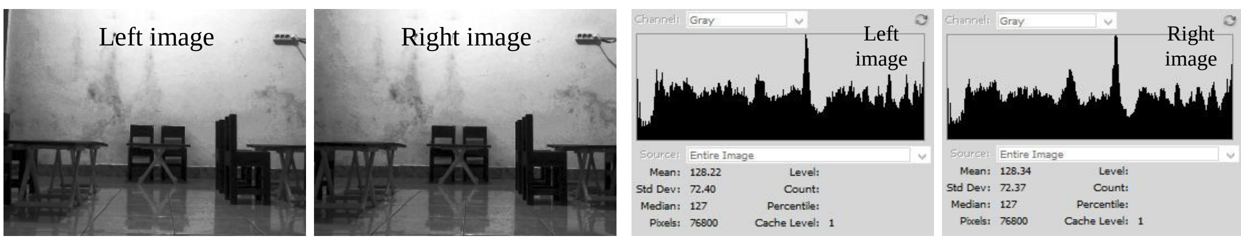

Figure 9. Left and right images after grayscaling process and its histogram

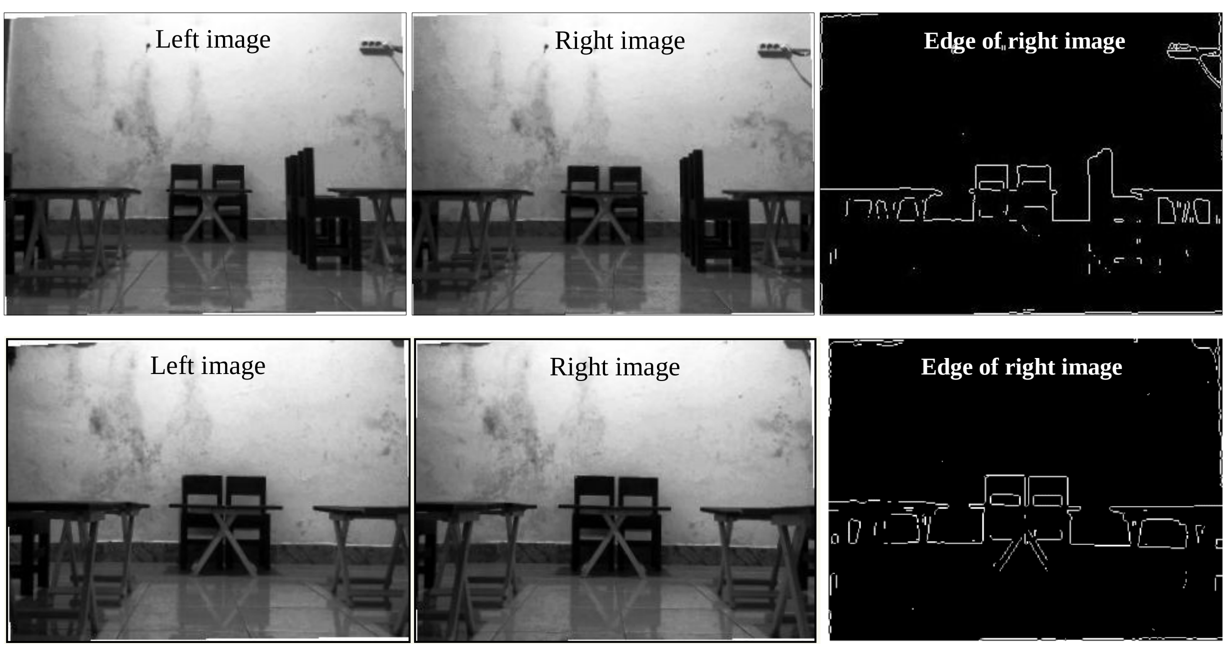

Figure 10. Rectified images and edge of right images

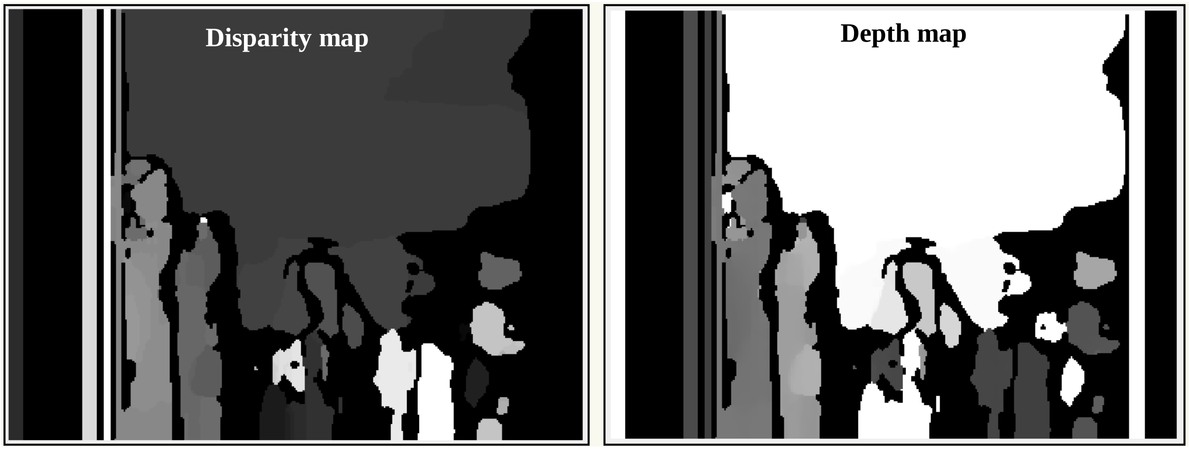

Figure 11. Disparity map and depth map from rectified images

Figure 12(a) and (b) show grid 3-1 and grid 3-2 of GED-Map that have built, while Table 1 and Table 2 show some of the pixel value of it. The full 25x25 of GED-map proposed in this paper shown in Figure 13. Every grid shows the results of edge detection of the obstacles that exist, including the value of the minimum distance from the detected distance obstacle in each grid. In Table 1, some pixel data from grid 3-1 equal to 64.4301 cm among another 48x64 data pixel of a grid. This value becomes the minimum value of detected object distance of this grid. Meanwhile, some pixel data from grid 3-2 equal to 111.22 cm in Table 2 and become the minimum value of detected object distance of this grid. For undetected or too far obstacles detected, the program gave a maximum value that is 500 cm. It may be found in some case of object distance measurement and shown on a particular grid. We set this value since our maximum distance in the environment is 500 cm. The GED-map was generated from the edge of the right image and the depth map. Only the right image to be processed and then compared with the depth map. When using the left the image, then the results of the experiment showed anomalies in the measurement of object distance toward the camera. The anomaly is meant that some measurements showed a considerable margin between the calculation results and the actual distance program. This is because the right image is used as a comparator in the development process of the disparity map. Some of the detected objects are not visible on the left image for their shifting positions of pixels in the right image matching (disparity value). Table 3 and Table 4 show our comparison of real distance measurement and calculated the distance by the program. Figure 14 shows the comparison's graph of calculated and real distance of detected object which is obtained from Table 3 and Table 4. In [2] the average error of feature points is 5.40 cm, whereas in this study was 3.82 cm. This result indicates that there has been a decrease in the measurement gap of 29.26% from the previous study.

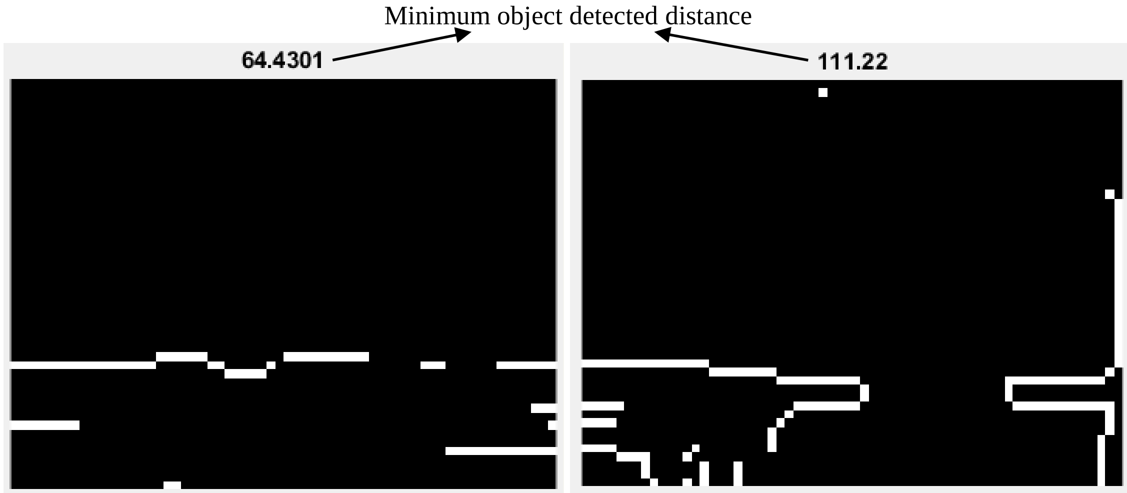

(a) (b)

Figure 12. (a) GED map on grid 3-1 (48 x 64 pixel) with minimum value 64.4301 cm
(b) GED map on grid 3-2 (48 x 64 pixel) with minimum value 111.22 cm

I. CONCLUSION AND FUTURE WORK

In this study, a new approach of a grid-edge-depth map building algorithm has been proposed utilizing a low-cost stereo camera. A pair of 320x240 pixels rectified grayscale images are used. Subsequently, Sum of Absolute Difference algorithm is utilized to build a disparity map. Depth map was built based on the disparity map and stereo parameter of the camera which is focal length and baseline. In order to achieve the best of distance measurement of the obstacle, we tried a few of disparity constant of SAD. We found that the best value of disparity constant is 48 and using this value the minimum distance of obstacles we could measure was 63 cm. Therefore, Sobel edge detection was implemented on the right rectified image. This image was used since it was a comparator image in disparity map process. Hereinafter our first focus method was the process of comparing the edge detection image and the depth map. Incorporating these processes results in a robust edge-depth information of the obstacle. Our next proposed method is dividing the edge depth into 5 rows and 5 column (25 grids). The size of each grid was 48 and 64 pixels respectively. Furthermore, the minimal depth of each grid was calculated as a minimally detected distance of the obstacles. The final result of this process is the grid-edge-depth map (GED map).

The size of each cell was 36 cm since the final view of GED map was 180 cm horizontally. This GED map has become the main contribution of this study.

The performance of GED map was evaluated by comparing its minimal calculated distance versus real distance of the obstacles. The result showed that the average error between the real distance and calculated distance was 3.82 cm. This result is 29.26% better from the previous study. We presumed the value is could be tolerated since the real distance measurement only used an integer and not using decimal as well as calculated by the program. The future work of this study is utilizing the GED map in mobile robot navigation purpose.

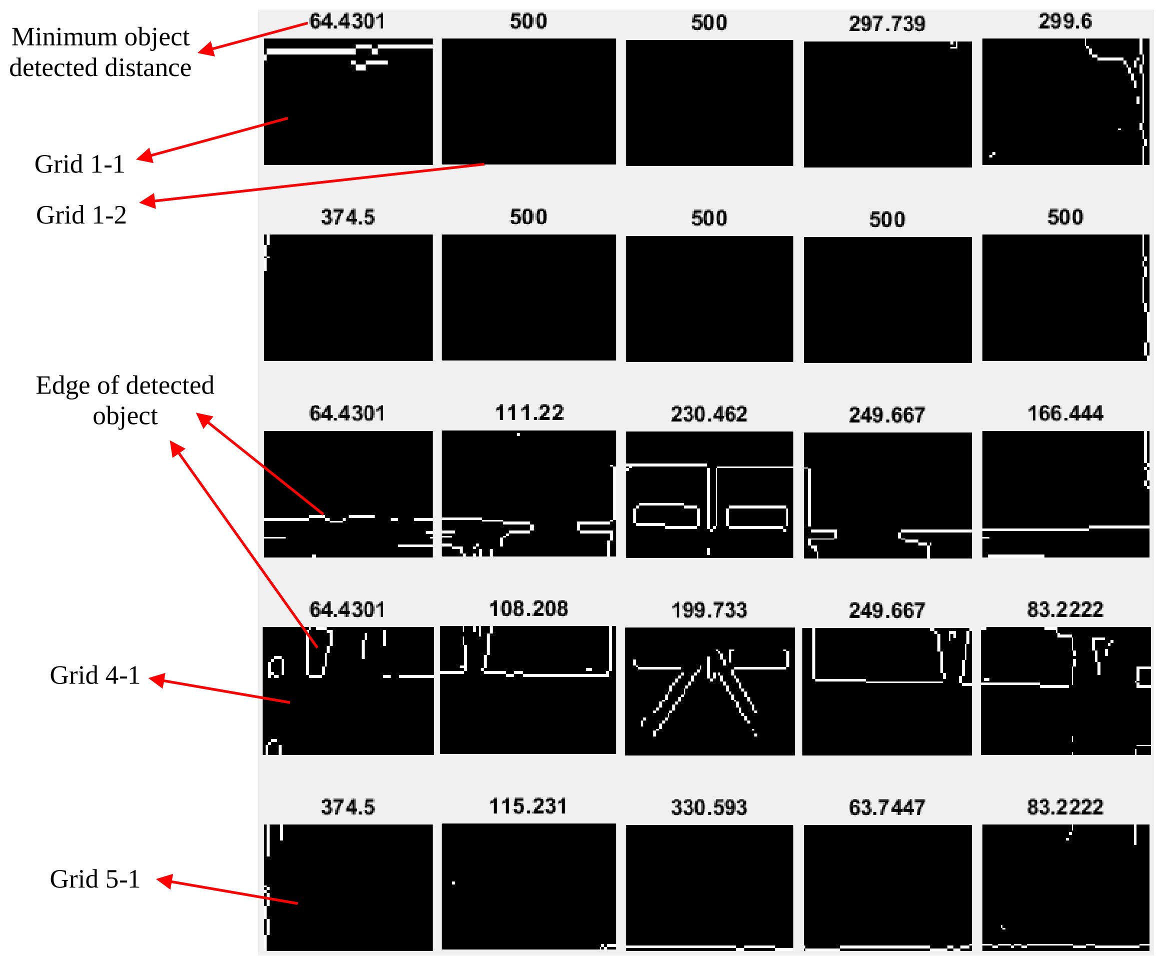

Figure 13. Full 25 x 25 Grid-Edge-Depth (GED) map with minimal object detected distance of each grid

Table 1. Grid 3-1 (55-64 of column and 130-144 of row)

ROW-COLUMN	55	56	57	58	59	60	61	62	63	64
130	500	500	500	500	500	123.5464	119.84	119.5411	119.5411	119.84
131	500	500	500	500	500	500	500	500	500	500
132	500	500	500	500	500	500	500	500	500	500
133	500	500	500	500	500	500	500	500	500	500
134	500	500	500	500	500	500	500	500	500	500
135	500	500	500	500	500	500	500	119.5411	119.5411	119.84
136	500	500	500	500	500	500	500	500	500	500
137	500	500	500	500	500	500	500	500	500	119.5411
138	500	500	500	500	500	500	500	500	500	500
139	500	500	500	500	500	500	500	500	500	500
140	64.43011	64.43011	64.43011	500	500	500	119.84	119.5411	119.5411	119.5411
141	500	500	500	500	500	500	500	500	500	500
142	500	500	500	500	500	500	500	500	500	500
143	500	500	500	500	500	500	500	500	500	500
144	500	500	500	500	500	500	500	500	500	500

Table 2. Grid 3-2 (65-74 of column and 130-144 of row)

ROW-COLUMN	65	66	67	68	69	70	71	72	73	74
130	500	500	500	500	500	500	500	500	500	500
131	119.84	119.84	119.84	119.84	119.84	119.84	119.2438	118.6535	118.3605	118.069
132	500	500	500	500	500	500	500	500	500	500
133	500	500	500	500	500	500	500	500	500	500
134	500	500	500	500	500	500	500	500	500	500
135	500	500	500	500	500	500	500	500	500	500
136	119.84	500	500	500	119.84	500	500	500	500	500
137	500	500	500	500	500	500	500	500	500	500
138	119.84	500	500	500	500	500	500	500	500	500
139	500	500	500	500	500	500	500	500	500	500
140	500	500	500	500	500	500	500	500	500	500
141	111.7389	111.4791	111.22	112	500	500	500	500	500	500
142	500	500	500	500	112	114.4057	114.4057	114.4057	500	500
143	500	500	500	500	500	500	500	114.1333	500	500
144	500	500	500	500	500	500	500	113.8622	500	500
145	500	500	500	500	500	500	500	500	113.8622	500

Table 3 Comparison of distance measurement (1)

Distance measurement (in centimeter)

Grid		Calculated distance	Real distance	Difference	Condition
1	1	500		500	No object
1	2	500		500	No object
1	3	500		500	No object
1	4	500		500	No object
1	5	500		500	
2	1	500		500	No object
2	2	500		500	No object
2	3	500		500	No object
2	4	500		500	No object
2	5	500		500	No object
3	1	102.44	100	2.44	
3	2	105.12	100	5.12	
3	3	216.91	214	2.91	
3	4	171.81	167	4.81	
3	5	114.13	110	4.13	
4	1	107.48	105	2.48	
4	2	107.96	105	2.96	
4	3	216.91	214	2.91	
4	4	167.02	165	2.02	
4	5	147.95	140	7.95	
5	1	500		500	No object
5	2	115.5	110	5.5	
5	3	500		500	No object
5	4	500		500	No object
5	5	182.96	180	2.96	

Table 4 Comparison of distance measurement (2)

Distance measurement (in centimeter)

Grid		Calculated distance	Real distance	Difference	Condition
1	1	500		500	No object
1	2	500		500	No object
1	3	500		500	No object
1	4	500		500	No object
1	5	500		500	No object
2	1	162	164	2	
2	2	500		500	No object
2	3	500		500	No object
2	4	500		500	No object
2	5	500		500	No object
3	1	108.7	104.5	4.2	
3	2	109.19	104.5	4.69	
3	3	204.86	200	4.85	
3	4	263.39	257	6.38	
3	5	239.49	235	4.49	
4	1	108.45	104.5	3.95	
4	2	140.99	137	3.99	
4	3	203.12	202	1.12	
4	4	238.49	237	1.49	
4	5	230.46	234	3.54	
5	1	123.87	115	8.87	
5	2	196.07	198	1.93	
5	3	194.86	196	1.14	
5	4	195.66	200	4.34	
5	5	500		500	No object

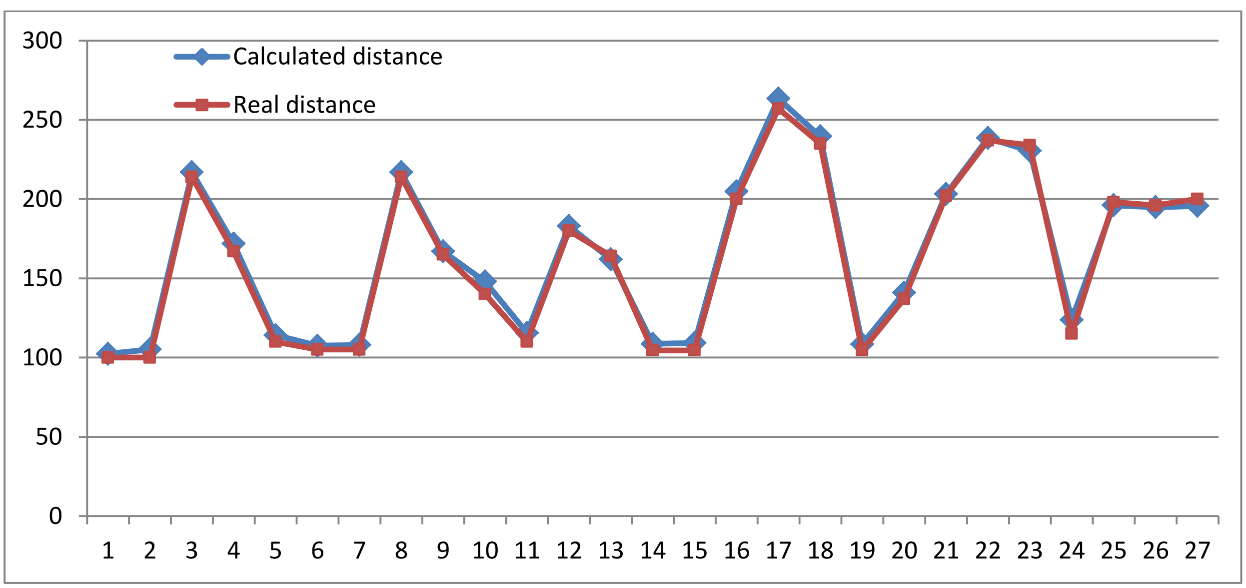

Figure 14. Comparison of calculated and real distance of detected object

REFERENCES

[1] S. Iizuka, T. Nakamura, and S. Suzuki, "Robot Navigation in Dynamic Environment Using Navigation Function APF with SLAM," in *2014 10th France-Japan/ 8th Europe-Asia Congress on Mecatronics (MECATRONICS2014- Tokyo)*, 2014, pp. 89–92.

[2] E. K. Kim, H. Cho, E. Jang, M. K. Park, and S. Kim, "Map Building of Indoor Environment using Laser Range Finder and Geometrics," in *IEEE International Conference on Advanced Intelligent Mechatronics (AIM)*, 2015, pp. 1–6.

[3] A. Alsaab and R. Bicker, "Behavioral Strategy for Indoor Mobile Robot Navigation in Dynamic Environments," *Int. J. Eng. Sci. Innov. Technol.*, vol. 3, no. 1, pp. 533–542, 2014.

[4] C. Ezequiel, "Real-Time Map Manipulation for Mobile Robot Navigation," M.S. Thesis, Department of Computer Science and Engineering, College of Engineering, University of South Florida, Tampa, FL, USA, 2013.

[5] R. L. Klaser, F. S. Osorio, and D. F. Wolf, "Simulation of an autonomous vehicle with a vision-based navigation system in unstructured terrains using OctoMap," *Brazilian Symp. Comput. Syst. Eng. SBESC*, pp. 177–178, 2014.

[6] D. Gonzalez-arjona, A. Sanchez, L. Fernando, and A. De Castro, "Simplified Occupancy Grid Indoor Mapping Optimized for Low-Cost Robots," *ISPRS Int. J. Geo-Information*, vol. 4, no. 2, pp. 959–977, 2013.

[7] T. Cao, Z. Y. Xiang, and J. L. Liu, "Perception in Disparity : An Efficient Navigation Framework for Autonomous Vehicles With Stereo Cameras," *IEEE Trans. Intell. Transp. Syst.*, vol. 16, no. 5, pp. 2935–2948, 2015.

[8] B. Rahmani, A. Harjoko, and T. K. Priyambodo, "Research of smart real-time robot navigation system," in *AIP Conference Proceedings*, 2016, vol. 1707.

[9] H. Soltani, H. D. Taghirad, and A. R. Norouzzadeh Ravari, "Stereo-Based Visual Navigation of Mobile Robots in Unknown Environments," in *20th Iranian Conference on Electrical Engineering (ICEE2012)*, 2012, pp. 946–951.

[10] X. Zhang and Z. Chen, "SAD-based stereo vision machine on a system-on-programmable-chip (SoPC)," *Sensors (Switzerland)*, vol. 13, no. 3, pp. 3014–3027, 2013.

[11] J. Heikkila and O. Silven, "A four-step camera calibration procedure with implicit image correction," in *Proceedings of IEEE Computer Society Conference on Computer Vision and Pattern Recognition*, 1997, pp. 1106–1112.

[12] R. A. Hamzah and S. I. M. Salim, "Software Calibration for Stereo Camera on Stereo Vision Mobile Robot using Tsai's Method," *Int. J. Comput. Theory Eng.*, vol. 2, no. 3, pp. 390–394, 2010.

[13] Y. M. Mustafah, R. Noor, H. Hasbi, and A. W. Azma, "Stereo Vision Images Processing for Real-time Object Distance and Size Measurements," in *2012 International Conference on Computer and Communication Engineering (ICCCE)*, 2012, pp. 659–663.

[14] R. H. Thaher and Z. K. Hussein, "Stereo Vision Distance Estimation Employing SAD with Canny Edge Detector," *Int. J. Comput. Appl.*, vol. 107, no. 3, pp. 38–43, 2014.

[15] J.-Y. Bouquet, "Camera Calibration Toolbox for Matlab," 2015. [Online]. Available: http://www.vision.caltech.edu/bouguetj/calib_doc/.

[16] H. Syahputra, A. Harjoko, R. Wardoyo, and R. Pulungan, "Improving disparity map of a specific object in a stereo image using camera calibration, Image rectification, and object segmentation," *Int. J. Appl. Eng. Res.*, vol. 9, no. 22, pp. 17939–17949, 2014.

[17] B. O. Kennedy, "Stereo Camera Calibration," University of Stellenbosch, 2002.

[18] C. McCormick, "Stereo Vision Tutorial (Part I)," 2014. [Online]. Available: http://mccormickml.com/2014/01/10/stereo-vision-tutorial-part-i/. [Accessed: 12-May-2016].

[19] S. Li, Y. Zhang, and P. Wang, "New Stereo Matching Method Based on Improved Back Propagation Algorithm," *Int. J. Smart Sens. Intell. Syst.*, vol. 8, no. 1, pp. 464–479, 2015.

[20] L. J. Liu, T. T. Zhang, G. P. Zhao, and L. J. Liu, "Detection of Moving Object by Fusion of Color And Depth Information," *Int. J. Smart Sens. Intell. Syst.*, vol. 9, no. 1, pp. 274–288, 2016.

[21] B. O. Sadiq, S. M. Sani, and S. Garba, "Edge Detection : A Collection of Pixel based Approach for Colored Images," *Int. J. Comput. Appl.*, vol. 113, no. 5, pp. 29–32, 2015.

[22] S. C. Abdullah, T. Ikai, Y. Dosho, H. Bin Yussof, and M. Ohka, "Edge Extraction Using Image and Three-Axis," *Int. J. Smart Sens. Intell. Syst.*, vol. 4, no. 3, pp. 508–526, 2011.